

Photon Correlation Spectroscopy in Particle Sizing

Walther Tscharnuter

Brookhaven Instruments Corporation, Holtsville,
NY, USA

Photon correlation spectroscopy (PCS) has become a powerful light-scattering technique for studying the properties of suspensions and solutions of colloids, macromolecules and polymers, that is absolute, non-invasive and non-destructive. This text explains the principles of the technique and describes the required instrumentation. It also discusses new developments in instrumentation, which may substantially impact on future applications of this technique. Proper sample preparation is of major importance for the accuracy and precision of the mean size and size distribution results and thus one section is dedicated to sample handling.

1 Introduction	1
2 History	1
3 Principles of Dynamic Light Scattering	2
3.1 Origin of Intensity Fluctuations	2
3.2 Detection Limits and Ranges	3
3.3 Time Domain Data Acquisition of a Random Signal (Correlation)	4
3.4 Data Reduction and Transformation	5
4 Sample Preparation	7
4.1 Concentration	7
4.2 Stability of Samples	8
4.3 Dust in the Sample	8
5 Instrument Performance	8
5.1 Efficiency of Data Acquisition	8
5.2 Result Verification	9
5.3 Standardization	9
6 Instrument Design for Dynamic Light Scattering	9
6.1 Light Source	9
6.2 Optical System	9
6.3 Detector System	9
6.4 The Digital Correlator	10
7 Examples of Dynamic Light Scattering Measurements	11
7.1 Particle Size Distributions	11
8 Comparison with Other Particle Sizing Methods	11
9 New Developments	12
9.1 New Correlator Developments	12
9.2 Solid-state Lasers	12
9.3 Fiber Optics	12
9.4 New Applications	12
10 Conclusion	13
10.1 Disadvantages	13
10.2 Advantages	13
List of Symbols	13
Abbreviations and Acronyms	14
Related Articles	14
References	14

1 INTRODUCTION

The acronym PCS is only one of several different names that have been used historically for this technique. The first name given to the technique was quasi-elastic light scattering (QELS) because, when photons are scattered by mobile particles, the process is quasi-elastic. QELS measurements yield information on the *dynamics* of the scatterer, which gave rise to the acronym DLS (dynamic light scattering). Another name, IFS (intensity fluctuation spectroscopy) was used by several authors in the past. Throughout this text the acronym DLS will be employed because its use has become more prevalent and presents a logical juxtaposition to SLS (static light scattering). Application of the DLS technique to particle sizing and commercial availability occurred only about seven years after the first size measurements⁽¹⁾ were made in 1972 merely to check the alignment of a multi-angle research light scattering system. Slowly, through the 1970s, DLS gained wide acceptance among experts in light scattering. This text is not meant to be exhaustive and emphasizes the application of DLS for particle sizing which relates to the *translational* motion (diffusion) of particles in liquids. However, DLS, by its nature, is not limited to this mode: any *time variable* parameter, such as the rotation or vibration of scattering centers, or fluctuations in the refractive index, entropy, thermal diffusivity etc. can be measured. The reader is referred to the extensive literature that exists on these subjects.

2 HISTORY

All materials scatter and absorb light and since the first light-scattering experiments described by Tyndall,⁽²⁾ SLS experienced major developments in the first half of the 19th century and is well described in the publications by Kerker.⁽³⁾ DLS theory is built upon the earlier foundation of classical light-scattering theory, which is usually dated

by Rayleigh's papers⁽⁴⁾ in 1871 on the scattering from a single particle small compared to the wavelength of light. Scattering from larger particles was added later and is known as Mie scattering, which gives the complete solution for spherical particles of any size. As early as 1908 the temporal fluctuations about the average scattered light intensity were identified with the motion of the particles and their diffusion coefficients. Einstein⁽⁵⁾ had already published the relationship between diffusion and size, so in principle the way was open for the birth of a new particle sizing technique. The fundamentals have been written about very often and these references should be consulted for a more complete treatment.^(6–26)

The history of experimental DLS begins with the advent of the laser. In the early 1960s Pecora⁽²⁷⁾ pioneered a new kind of light scattering: *time dependent* light scattering. He showed that, by analyzing the frequency distribution of the intensity fluctuations of light scattered from suspensions of macromolecules, information can be obtained about the translational and rotational diffusion coefficients of the macromolecules. Initially DLS was used to measure the diffusion coefficient of macromolecules, from which a hydrodynamic size was calculated. A few industrial users tried this technique for submicron particle sizing, mostly to replace transmission electron microscope (TEM) measurements in quality control (QC) applications. During the second half of the 1970s improvement of digital correlators and the introduction of several algorithms for analyzing decay time distributions were seen. Measurements that had taken months to set up and hours to make, were now reduced to minutes. Bertero et al.^(28,29) published a fundamental paper in 1984 that derived the limiting conditions for the resolution of the “noisy” sum of an unknown number of exponentials based on information theory. The advent of highly efficient nonlinearly spaced correlators ushered in a steep ascent of the utility of DLS particle sizing in the mid-1980s, and the emerging fast computers speeded up data handling. Unfortunately, the pretty pictures and rapidly achieved size distribution results often mask the real underlying limitations that are imposed by the physics of the technique.

3 PRINCIPLES OF DYNAMIC LIGHT SCATTERING

3.1 Origin of Intensity Fluctuations

Colloidal sized particles in a liquid undergo random (“Brownian”) motion owing to multiple collisions with the thermally driven molecules of the liquid. The scattered light intensity from these diffusing particles will fluctuate in time, thus carrying information about the diffusion

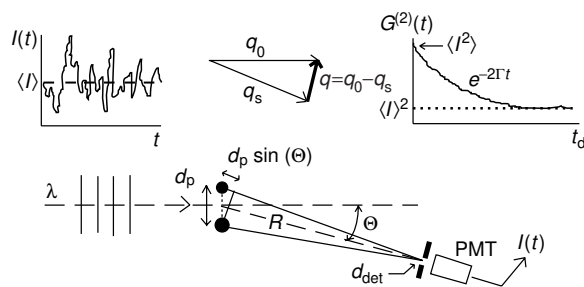


Figure 1 The basics of DLS.

coefficient of the particles. Cummins, Knable and Yeh⁽³⁰⁾ demonstrated a method to determine the spectrum of light scattered from a dilute suspension of polystyrene spheres by employing novel optical techniques. Following is a description of the basic physics of the DLS technique and of the instrumentation employed in these measurements. The approach used is not intended to be exhaustive; for more details, the literature presented at the end of this article should be consulted. The NATO proceedings edited by Cummins and Pike^(7,8) are particularly valuable. The volume edited by Chu⁽⁹⁾ conveniently collects many of the major papers together. The article by Ford⁽²⁵⁾ provides an excellent introduction to many of the practical aspects of the technique and the book by Wyn Brown⁽²⁶⁾ contains many valuable contributions to various data transformation methods. Equation (1) describes the time averaged scattered intensity $\langle I(q) \rangle$ in terms of particle parameters (also see Figure 1)

$$\langle I(q) \rangle = KNM^2 P(\Theta) B(c) \quad (1)$$

$$q = \frac{4\pi n}{\lambda_0} \sin \left(\frac{\Theta}{2} \right) \quad (2)$$

where q is the magnitude of the scattering vector, Θ is the scattering angle, λ_0 is the wavelength of the laser in vacuo and n is the refractive index of the suspending liquid; K is an optical constant, N is the number of scattering particles, M is the mass of a particle, $P(\Theta)$ is the particle form factor, and $B(c)$ is the concentration factor. The terms M^2 and $P(\Theta)$ are of particular importance for the determination of size distributions. The central concept in DLS is as follows: the diffusion of the scatterers (Brownian motion) causes the phases of the fields scattered from each of them to change with time so that the *total* scattered intensity will fluctuate with time owing to constructive and destructive interference. The source of the intensity fluctuations can be understood with reference to Figure 1. A laser beam of wavelength λ is incident on two identical particles. Light scattered by the particles is received by a photo multiplier tube (PMT) and it can be readily seen that the pathlength

difference between the scattered waves is $d_p \sin(\Theta)$. When this pathlength difference is equal to an integer multiple of wavelengths $d_p \sin(\Theta) = m\lambda$, the wavelets will arrive at the detector *in phase* (constructive interference), i.e. the total intensity will be twice that from a single particle. When the pathlength difference is a half integer multiple of wavelengths $d_p \sin(\Theta) = \lambda/2, 3\lambda/2, 5\lambda/2, \dots$, then the two wavelets will be exactly *out of phase* (destructive interference), i.e. the resulting intensity will be zero. The relative positions and orientations of the particles undergo Gaussian random changes in time (Brownian motion). The result is a total intensity which fluctuates in time from zero to double the single particle scattered intensity. In a real experiment there are perhaps $\sim 10^8$ particles in the scattering volume, and the total intensity is the result from the interference between the scattered fields from all of these. As a consequence, the intensity $I(t, q)$, as seen by the detector, will be a randomly fluctuating signal as shown. Its well-defined mean value, $\langle I(q) \rangle$, is the quantity measured in a SLS experiment. The intensity fluctuations are not readily observed because they occur on a rapid timescale (10^{-6} – 10^{-3} s) and because they take place only at a point (Ford⁽³¹⁾). The first condition necessitates a high-speed detection and recording system. The second condition is of fundamental importance in DLS measurements because it determines the limiting properties of the optical system. When the light scattered from a suspension of colloidal particles undergoing Brownian motion is projected onto a screen or wall, a granular pattern (“speckles”, bright and dark patches) is observed. The integral intensity appears constant. However, the intensity of each individual speckle changes randomly in time from very dark to very bright. The intensity of adjacent spots also fluctuates, but independently. Thus the largest spread in intensity (the fluctuations) will be obtained by looking at exactly only one spot. As the number of spots observed increases, the magnitude of the fractional intensity *fluctuations* will decrease, because the spots’ intensities fluctuate independently and the high probability of one spot’s intensity increasing and another’s decreasing yield small integral fluctuations,

even though the *total time averaged* intensity increases by observing several speckles simultaneously. The intensity fluctuations will be in phase, or coherent, if the light is detected over one “coherence area” (one speckle) the size of the coherence area. For the configuration shown in Figure 1, where a scattering volume of diameter d_p is a distance R away from a detector, the size of the coherence area A_{coh} ⁽¹⁵⁾ is given by Equation (3):

$$A_{\text{coh}} = \frac{4\lambda^2 R^2}{\pi d_p^2} \quad (3)$$

The area of the detector is given by Equation (4)

$$A_{\text{det}} = \frac{\pi d_{\text{det}}^2}{4} \quad (4)$$

and if this is set equal to A_{coh} , the size of the detector that is sufficient to see only one coherence area may be calculated. For a typical arrangement with $\lambda = 475$ nm (HeNe laser wavelength in water), $R = 15$ cm and d_p (the diameter of the scattering region) = 0.2 mm, the diameter of the detector d_{det} will be ~ 0.9 mm for one coherence area, i.e. a detector aperture of ~ 0.9 mm is required to see one spot and achieve the maximum signal-to-noise ratio (S/N). Since there is no advantage for most experimental conditions in collecting more than one coherence area, it is important to have the maximum intensity scattered into a small area. This is achieved by tightly focusing the incident beam to decrease d_p and increase the size of the coherence area (Equation 3).

3.2 Detection Limits and Ranges

Several experimental conditions must be met for the applicability of the relevant physics for SLS and DLS techniques in general, and particle sizing in particular (also see Table 1 in section 4):

3.2.1 The Optical Mixing Mode

Any measurement must use exclusively one of the following three optical mixing modes:

Table 1 Summary of measurement problems

Condition	Cause	Effect
Multiple scattering present	Concentration too high	Measured sizes <i>too low</i>
Stray light present	Light reflections	Measured sizes <i>too large</i>
Dust present	Sample preparation	Incorrect size distribution
Duration too short	Operator impatience	Unrepeatable results
Ergodicity not assured	Nature of the sample	Unrepeatable results
Size range exceeded	Operator ignorance	Unrepeatable results
Sample not stationary	Aggregation, sedimentation	Unrepeatable, averaged results
Sample preparation	Impatience or ignorance	Incorrect or unrepeatable results

- Self beating: the scattered light mixes on the photo multiplier cathode with itself.
- Homodyning: the scattered light mixes with a strong signal from the same laser. This signal, a *local oscillator*, must have the *same* frequency, must be at least an order of magnitude higher than the scattered light, and must be in phase with it. If the auto correlation function (ACF) contains a mix of self beating and homodyning, the calculated sizes are invalid. Unfortunately there is no easy way to recognize this problem when it is present. Only one commercially available instrument employs the *homodyning* mode for particle sizing.⁽³²⁾
- Heterodyning: the scattered light mixes with a strong signal of a *different* frequency (a local oscillator), which is generated either by frequency shifting the same laser or by using a laser beam with a different frequency.

It should be noted that in the literature the terms self-beating and homodyning are frequently used interchangeably and homodyning is confused with *heterodyning*. Here these terms are used according to their true definitions: DLS-based particle sizing applications operate almost exclusively in the self-beating mode, *homodyning* is used rarely and *heterodyning* is not employed at all. However, DLS Doppler (velocimetry) experiments are conducted almost exclusively in the heterodyne mode.

3.2.2 Concentration

The concentration must be sufficiently low so that in Equation (1) $B(c) = 1$ and *multiple scattering* (see below) is avoided, but also must be sufficiently high to prevent signal distortions due to number fluctuations. The number of the particles in the scattering region must always be sufficiently high to maintain a constant $\langle I(q) \rangle$ (Equation 1).

3.2.3 Multiple Scattering

Unless the concentration is vanishingly small, any scattered photon has a non-zero probability to be scattered again while traveling through the sample. The ACF of such multiple scattered light decays faster, yielding an apparent smaller particle size. Thus the sample concentration must be kept sufficiently low and/or the optical path must be sufficiently short to avoid multiple scattering.

3.2.4 Ergodicity

All particles must have an equal opportunity to be measured. This condition is sometimes difficult to meet if

the diffusion coefficient of the scatterers is very low, see Pusey.^(19,33)

3.2.5 Stationary Process

Scattering conditions must not change during the measurement.

3.2.6 Stray Light

Stray light must be avoided to prevent inadvertent homodyning (see section 3.2.1) and commonly determines the low limit of the angular measuring range.

3.2.7 Sample Preparation

The term M^2 in Equation (1) predicts the scattered intensity to be $\propto d^6$. Consequently a few large particles (commonly called “dust”), will overwhelm the desired signal (see section 4).

3.2.8 Size Range

The DLS technique is commonly employed in the range of 0.002 to 2 microns. The low limit is usually determined by the available laser power. The high limit results from sedimentation and number fluctuations due to the low number of large particles that fit into the small scattering volume.

3.2.9 Measurement Duration

The typical range is from 1 to 10 minutes, depending on $\langle I(q) \rangle$.

3.3 Time Domain Data Acquisition of a Random Signal (Correlation)

To see how the signal $\langle I(q) \rangle$ changes with time it is convenient to compute its ACF. The *intensity* ACF is described by Equation (5):

$$G^{(2)}(t_d) = \frac{1}{N} \sum_{i=1}^N I(t_i)I(t_i - t_d) = \langle I(t)I(t - t_d) \rangle \quad (5)$$

The angle brackets indicate a time average, N is the number of samples and t_d is the time delay between the samples. Experimentally, $G^{(2)}(t_d)$ is determined by recording $I(t)$ at time intervals much shorter than the timescale of typical fluctuations and accumulating the products of the intensities as a function of (t_d) . For a dilute suspension of monodisperse spheres (e.g. latex particles), $G^{(2)}(t_d)$ can be written as Equation (6):

$$G^{(2)}(t_d) = B + f \times e^{-2\Gamma t_d} \quad (6)$$

where $B = \langle I \rangle^2$ (Figure 1) is the baseline, f is an instrumental constant and 2Γ is the reciprocal of the decay time τ . $G^{(2)}(t_d)$ is normalized by dividing Equation (6) into the base B , yielding in Equation (7) the normalized intensity ACF $g^{(2)}(t_d)$. For Gaussian statistics Glauber⁽³⁴⁾ derived Equation (7) via the Siegert relation⁽³⁵⁾

$$g^{(2)}(t_d) = 1 + a[g^{(1)}(t_d)]^2 \quad (7)$$

relating the electric field ACF $g^{(1)}(t_d)$ to the measured intensity ACF $g^{(2)}(t_d)$, and a is an instrumental constant that is now between 0 and 1. It should be noted that any photoelectric detector is sensitive to the intensity of light, which is the square of the field amplitude. The normalized electric field ACF $g^{(1)}(t_d)$ may be written as Equations (8) and (9):

$$g^{(1)}(t_d) = G_0 e^{-\frac{t_d}{\tau}} \quad (8)$$

$$\Gamma = \frac{1}{\tau} = D_T q^2 \quad (9)$$

where $\tau = 1/\Gamma$ is the decay constant and D_T is the translational diffusion coefficient of the spheres, and G_0 is the intercept of the exponential function, $g^{(1)}(t_d = 0)$. In the case of measurements on dilute monodisperse spheres, the intensity ACF will be a simple exponential function as shown in Figure 2. The significant parameter in Equation (8) is τ , which is invariant to the scattered intensity $\langle I(q) \rangle$. Thus, for DLS-based measurements, the absolute intensity is of secondary importance, as long as it is sufficiently large to complete the experiment within the lifetime of the operator or the stability of the sample, whichever comes first. Measurements in the frequency domain yield the same information; in Equation (10) the power spectral density $S(w)$ is the Fourier transform of

$g^{(1)}(t_d)$ and has the shape of a Lorentzian.

$$S(w) = \langle I(t) \rangle \frac{(2\Gamma)^2}{w^2 + (2\Gamma)^2} \quad (10)$$

The relationship between Γ and τ is defined in Equation (9), from which the particle diffusion coefficient D_T can be calculated. Finally in Equation (11), for spheres, D_T is related directly to their hydrodynamic radius r_h by the Stokes–Einstein relationship

$$D_T = \frac{k_B T}{6\pi\eta(T)r_h} = \frac{k_B T}{3\pi\eta(T)d_h} \quad (11)$$

Here k_B is the Boltzmann constant, T is the absolute temperature (Kelvin) and $\eta(T)$ is the viscosity of the suspending liquid (the viscosity is strongly temperature-dependent, requiring a constant temperature throughout a measurement); r_h and d_h are the hydrodynamic radius and diameter respectively; these values are almost always larger than the dry particle diameter owing to the “double layer” that forms around charged particle surfaces. The counter-ions around the particle form a diffuse region which moves with the particle. An important parameter for colloidal stability, the “zeta potential”, is defined at approximately the location of the shear plane (the outer “edge” of the diffuse double layer).

3.4 Data Reduction and Transformation

The simplest case involves a single exponential decay for a monodisperse sample as shown in Figure 2 (owing to the logarithmic time axis, the ACF is ‘S’ shaped). After dividing the correlation coefficients into the baseline and subtracting 1, the remaining part, $G_0 e^{-\Gamma t}$, is fit using a least-squares technique. The value of G_0 typically varies from 0.1 to 0.9 depending on the optical configuration. G_0 is a maximum when the coherence criterion is met. The particle diameter is calculated from D_T in Equation (11). Typical results on latex spheres show the technique is as reliable as an electron microscope on monodisperse samples or latex spheres. The size calculated from Equation (11) is a hydrodynamic diameter.

3.4.1 Monodisperse Distribution

The results for monodisperse samples can be compared directly with other techniques since there is only one “average” diameter. For nonspherical particles either the results can be interpreted in terms of an equivalent sphere diameter equal to the Stokes–Einstein hydrodynamic diameter, or the diffusion coefficient can be interpreted in terms of ellipsoids of revolution.⁽³⁶⁾ This requires either independent knowledge of one dimension or their ratio,

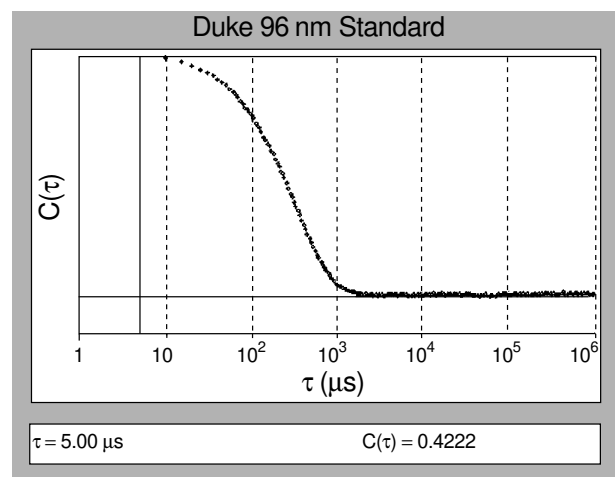


Figure 2 Semi-log plot of a single mode ACF.

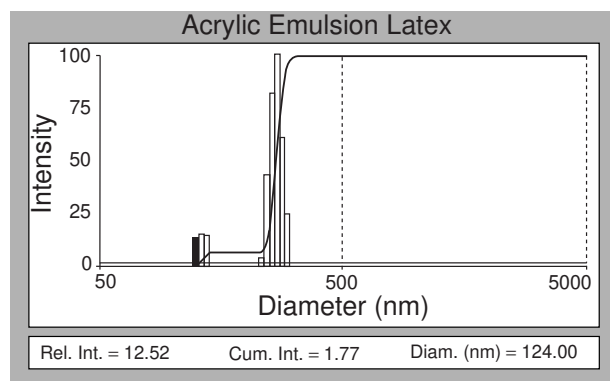


Figure 3 Bimodal distribution of an emulsion.

or angular measurements from which, in favorable cases, both dimensions can be calculated.⁽³⁷⁾

3.4.2 Polydisperse Distribution

The interpretation of data from polydisperse samples (Figure 3) is considerably more difficult. Since the technique does not count single particles, size distribution information must be obtained from the deconvolution of the sum over all the single exponentials contributing to the measured ACF. The general deconvolution of a sum of single exponentials is difficult. The problem may be summarized by Equations (12) and (13) which define the normalized field ACF $g^{(1)}(t_d)$ as the sum of m particle sizes, each of which contributes $G(\Gamma_i)$ for the i -th size class.

$$\begin{aligned} g^{(1)}(t_d) &= G(\Gamma_1) e^{-\Gamma_1 t_d} + G(\Gamma_2) e^{-\Gamma_2 t_d} \\ &\quad + G(\Gamma_3) e^{-\Gamma_3 t_d} + \dots \\ &= \sum_{i=1}^m G(\Gamma_i) e^{-\Gamma_i t_d} \end{aligned} \quad (12)$$

Here Γ_i is the value as defined in Equation (9). For the limit of $\Gamma_{i+1} - \Gamma_i = \Delta\Gamma = 0$, $g^{(1)}(t_d)$ is defined in Equation (13) by integrating over the entire range of particle sizes

$$g^{(1)}(t_d) = \int_{\Gamma_{\min}}^{\Gamma_{\max}} G(\Gamma) e^{-\Gamma t_d} d\Gamma \quad (13)$$

where $G(\Gamma)$ represents the distribution of line widths due to the distribution of particle sizes. Γ_{\min} and Γ_{\max} define the range of line width; in principle, $\Gamma_{\min} = 0$ and $\Gamma_{\max} = \infty$. It is easy to calculate $g^{(1)}(t_d)$ from a known size distribution $G(\Gamma)$, but exceedingly difficult to perform the inverse transformation to extract $G(\Gamma)$ from $g^{(1)}(t_d)$. Equation (13) belongs to a class of linear transformations (Laplace) that are known to be ill-conditioned. In the presence of any noise, many different solutions

for the functional form of $G(\Gamma)$ are possible. A repeat measurement on the same sample will yield a slightly different $g^{(1)}(t_d)$ with a slightly different noise contribution, resulting in a different $G(\Gamma)$ and hence in a different size distribution $G(d)$. This behavior can render the results of a DLS instrument apparently “not repeatable”. For these fundamental reasons of physics DLS will not become a high-resolution technique for particle sizing. Numerical solutions of Equation (13) were attempted by Chu and Gulari,⁽³⁸⁾ McWhirter and Pike,⁽³⁹⁾ McWhirter⁽⁴⁰⁾ and Ostrowsky and Pike⁽⁴¹⁾ have demonstrated that $G(\Gamma)$ can be calculated at exponentially spaced delay times. The method, called *exponential sampling* introduces ϖ_0 as a parameter that limits the resolution of $G(\Gamma)$ for a given noise level in Equation (14).

$$\Gamma_{i+1} = \Gamma_i e^{\frac{\pi}{\varpi_0}} \quad (14)$$

Here ϖ_0 is the largest value for a fixed noise content of $g^{(1)}$ and therefore defines the best possible resolution for Γ_i and Γ_{i+1} . Example: if $\varpi_0 = 3.14$, $\Gamma_{i+1}/\Gamma_i = 2.71$; if Γ_{i+1} corresponds to a size of, e.g. 500 nm, the next neighboring peak cannot be closer than 184 nm ($500/2.71$) or 1050 nm ($500 \cdot 2.71$). If the inversion routine asks for a higher resolution than can be supported by the ACF, the Gamma distributions will exhibit more and more artifacts such as additional maxima and negative values for $G(\Gamma)$. The practical limit for the ratio Γ_{i+1}/Γ_i is 2. It is important to note, that this resolution cannot be exceeded by any transformation routine without imposing additional, a priori imposed, constraints. The most commonly applied constraints are non-negativity (only zero or positive $G(\Gamma)$ are allowed), range limitations and force fits to specific distribution models (log-normal, bimodal). Provencher^(42,43) has developed an effective inversion software package, CONTIN, which is a generalized Inverse Laplace Transform with constraints and parsimony. CONTIN contains a non-negative least square routine (NNLS), that may be used effectively as a fast executing stand-alone program to obtain rapid size distributions in real time during data acquisition.⁽⁴⁴⁾ Several other inversion programs are in use by practitioners, e.g. “Maximum entropy”,⁽⁴⁵⁾ “REPES”,⁽⁴⁶⁾ and “single value decomposition”.^(47,48) H. Ruf⁽⁴⁹⁾ investigated the errors that are introduced into the inversion process owing to normalization errors. Aside from the noise content of the ACF, baseline errors contribute a significant amount of ambiguities to any of the transformation routines and repeated, iterative, normalizations of the ACF can improve the stability of the results. The above approaches show that only a few parameters of the distribution can be calculated from typical experimental measurements of the correlation function. Present work on these advanced techniques is focusing on the separation of only two peaks

in a size distribution, the size ratio of which is at least 2 : 1. Thus DLS measurements must be considered as relatively insensitive to the particular size distribution and only a few moments of the distribution can be obtained, except for monodisperse samples, for which the technique works extremely well.

3.4.3 Cumulants

The most widely used and simplest data analysis technique to apply is the *method of cumulants*.^(50,51) The method proceeds by expanding Equation (13) about an average line width $\langle \Gamma \rangle$, to give Equation (15):

$$\ln[a_0 g^{(1)}(t_d)] = a_0 - \langle \Gamma \rangle t_d + \frac{\mu_2}{2} t_d^2 - \frac{\mu_3}{6} t_d^3 + \dots \quad (15)$$

where a_0 is a constant and $\langle \Gamma \rangle$, μ_2 , etc. are moments of the line width distribution $G(\Gamma)$. In practice only the first two moments are obtained with certainty, and care must be taken to limit the range of t_d such that higher order terms are negligible. Before the advent of non-linearly spaced correlator channels this used to be difficult for broad distributions. This technique has the advantage that no assumption about the form of the distribution is necessary, and, under the correct experimental conditions described earlier, the moments are well defined and useful parameters. It has been shown by Brown, Pusey and Dietz⁽⁵⁰⁾ that (Equation 16):

$$\langle \Gamma \rangle = \langle D_T \rangle q^2 \quad (16)$$

where $\langle D_T \rangle$ is given by Equation (17),

$$\langle D_T \rangle = \frac{\sum N_i M_i^2 P_i(\Theta) D_i}{\sum N_i M_i^2 P_i(\Theta)} \quad (17)$$

NM^2P is the time-averaged intensity weighting factor (Equation 1) for the contribution of D in the i -th size class. The sum is over all the particles contributing to the scattering, and it has been assumed that the measurements have been made or will be extrapolated zero concentration. If not, the interparticle interference term $B(c)$ must be included in Equation (17). It has also been assumed that the optical constant K in Equation (1) is the same for all particles independent of size. K includes the refractive index increment (change of solution refractive index with particle concentration). So the assumption of a constant K means assuming a sample of homogeneous composition independent of size. For Rayleigh scatterers ($d \ll \lambda$) and for all particles where measurements have been extrapolated to zero angle, where $P(\theta) = 1$, and

$$\langle D \rangle = \langle D \rangle_z = \frac{\sum N_i M_i^2 D_i}{\sum N_i M_i^2} \quad (18)$$

Here $\langle D \rangle_z$ is the well-defined z -average diffusion coefficient (z -weighting means the next higher weighting after volume). Thus, for spheres, where $M^2 \propto d^6$, the average particle size obtained is (Equation 19),

$$\frac{1}{d_z} = \frac{\sum N_i d_i^5}{\sum N_i d_i^6} \quad (19)$$

Here d_z is the inverse, z -average diameter and N_i is the number of particles in the i -th size class. The second moment in the cumulant analysis, μ_2 in Equation (20) yields (after extrapolation to zero concentration and zero angle)

$$\mu_2 = \langle D_z^2 \rangle - \langle D_z \rangle^2 \quad (20)$$

which is the *variance* of the z -average diffusion coefficient distribution. For spherical particles the first term can be related to the inverse square, z -average diameter, $\langle (1/d^2)_z \rangle$. This technique has the advantage that no assumption about the form of the distribution is necessary, and the moments are well defined and useful parameters. A convenient polydispersity index is defined as Q in Equation (21)

$$Q = \frac{\mu_2}{\langle \Gamma \rangle^2} = \frac{\langle D_z^2 \rangle - \langle D_z \rangle^2}{\langle D_z \rangle^2} \quad (21)$$

where μ_2 , $\langle \Gamma \rangle$ and $\langle D_z \rangle$ are defined in Equations (20), (16) and (17) respectively. For QC measurements the exact interpretation of data is not usually of primary importance. In this case, measurement at one angle, usually 90° , is sufficient to establish an apparent average size and apparent measure of the width of the size distribution. Monitoring changes in these two parameters may be all that is required. In many cases the distribution is known to be log-normal or reasonably close to one; Thomas⁽⁵²⁾ showed that in this case the two parameters μ_2 and $\langle \Gamma \rangle$ may be mathematically transformed to geometric standard deviation and mass mean diameter, the two parameters that define a log-normal function. Such transformations are not limited to log-normal functions but can be performed for any other two parameter distribution. It is important, however, not to forget that this function may or may not resemble the real particle size distribution, although it definitely will produce a “nice” looking display on the computer screen.

4 SAMPLE PREPARATION

4.1 Concentration

Concentration effects manifest themselves in two fundamentally different ways:

4.1.1 Multiple Scattering

Even if D_T is indeed independent of c , the “particle size” will be reported as too small, because the correlation is lost on a shorter timescale for multiple scattered photons. A comparatively new set of experiments has been successful in analyzing the dynamics of multiple scattered photons from concentrated samples (see section 9).

4.1.2 Particle–Particle Interaction

The apparent viscosity depends on particle–particle interaction. In sufficiently high concentrations where particles experience significant interactions, the calculated particle size is different from those obtained under infinite dilution conditions. There is a large amount of physics to be learned from such experiments, as long as the instrument is capable of eliminating multiple scattering effects, so that the true functional form of $D_T(c)$ can be obtained and the theories for particle–particle interaction can be investigated (see section 9).

4.2 Stability of Samples

The scattering environment must not change during the measurement. Sometimes this is difficult or impossible to accomplish owing to the presence of changing chemical and/or physical parameters in the sample (chemical reactions, aggregation, temperature). If those changes are the objects of investigation, the experiment duration must be kept sufficiently small compared to the characteristic times of the reactions. Under most operating conditions, however, an unstable sample is the result of inappropriate sample preparation. The following describes a general approach to solving the sample preparation problem as it relates to particle sizing.

4.2.1 Coagulation

Physics predicts (van de Waals forces) that, allowing for a sufficiently long time, any colloidal dispersion will coagulate, be it seconds, minutes or years. Thus the problem to be solved can be stated very simply: how long is stability required? For particle sizing typically 30 minutes are sufficient, but for a commercial product a long shelf life is imperative. It will exceed the scope of this text to dwell on any details, but fortunately even only superficial attention to some basic surface chemistry will result in meaningful particle size measurements. Under most operating conditions an unstable sample is the product of inappropriate sample preparation. The following describes a general approach to sample preparation as it relates to particle sizing.

4.2.2 Hydrophobic or Hydrophilic Sample Surfaces?

Sprinkling a few particles on the surface of the water will rapidly reveal their properties: hydrophilic particles will rapidly disperse in the water, hydrophobic types will stay on the surface. The former will generally merely require a stabilizing surfactant, whereas the latter often can be converted into a hydrophilic system by creating a paste of the particles and methyl alcohol.

4.2.3 Zeta Potential

The “zeta potential” of particles (a measurement of the electrostatic repulsion between particles) is a good, but certainly not the only, predictor of the stability of a suspension. Unless the sample is sterically stabilized, a low zeta potential increases the probability for aggregation within a short time; thus the determination of this parameter is very important. Frequently a simple change of the pH value is all that is required to achieve a stable suspension. Further information about electrophoretic mobility (zeta potential) and the stability of colloidal systems can be found in a book by Hunter.⁽⁵³⁾

4.3 Dust in the Sample

The appropriate use of surfactants to avoid aggregation, filtering, centrifugation, ultrasonication, cleaning of sample cells and the use of deionized and filtered water are of utmost importance for any serious size measurement. Dust will not only cause huge intensity spikes and distort the raw data but can also introduce unintentional homodyning to the self-beating mode by actually creating a local oscillator. Nonaqueous (nonpolar) liquids do not attract “dust” as much and are easier to clean, but sample preparation is often more complicated. Filtering of all liquids, especially water, and thorough cleaning of all sample cells as well as pipets, syringes, etc. are always required. DLS instruments, by their nature, will collect at least the dark counts from a detector, always resulting in some nonzero ACF. The computer will happily calculate a “result”, regardless of the quality of the signal, thereby creating insidious and serious problems if any of the above listed conditions is violated. Table 1 shows a compilation of the most common error sources in DLS particle size measurements.

5 INSTRUMENT PERFORMANCE

5.1 Efficiency of Data Acquisition

The ACF consists of many product terms which asymptotically converge to a steady function. The overall

optimization of the statistics begins with the efficient launching of the laser beam, the collection of the scattered photons by bulk or fiber optics and the quantum efficiency (QE) of the detector. All available photon pulses should be utilized by the optics and the electronics in order to achieve the best possible statistics in the least amount of time. Here the design of correlators that do not require any prescaling presents a significant advance in this technology. Modern correlators do not depend on raw computer speed for data collection, but in QC applications the “throughput”, which includes data reduction, display, storage and possible statistical process control (SPC) depends on the performance of the attached data processor.

5.2 Result Verification

DLS results are sometimes not easy to interpret since there always will be some result displayed. Several conditions can be stipulated for the correctness of the results:

- *repeatability*: this is a necessary, but not a sufficient condition;
- *invariance of the size distribution* to the delay time range, as long as the smallest range covers the set of decay times;
- *invariance of the peak positions* to the chosen range of particle sizes;
- *no peaks at the extremes* of the chosen size range;
- *consistency of the results* with the physical and chemical properties of the particles;
- *consistency of the results* with other sizing techniques. If data transformations are required they must be evaluated very carefully (see section 3).

5.3 Standardization

The International Organization for Standardization (ISO) published a draft paper that proposes to establish “standard” methods for the application of the DLS technique to the measurement of particle size distribution of samples with specified properties. Details of the proposal can be found in the publications of the

subcommittee.⁽⁵⁴⁾ It should be noted that this publication is just a proposal subject to amendments. It presents a framework of design rules for DLS-based particle sizing that should yield results which are invariant to specific instruments or operators around the world.

6 INSTRUMENT DESIGN FOR DYNAMIC LIGHT SCATTERING

A typical DLS system may be broken down into several functional components which will be discussed separately. These are a light source, an optical system, a detector system and a digital correlator.

6.1 Light Source

Practical requirements for a sufficiently intense light source demand a narrow-band, polarized, monochromatic, CW laser. Table 2 summarizes the popular options available.

DPSS have become widely available within the last few years. Their wavelength is typically 532 nm (frequency doubled from powerful 1064 nm diode lasers) and their other properties match well with the requirements of DLS instruments.

6.2 Optical System

A lens focuses the laser beam down into the sample which is enclosed in a temperature-controlled scattering cell surrounded by a refractive index matching liquid. The scattered light is focused onto a PMT at an angle θ by another lens. Systems like this are constructed on a precision turntable with a stepper motor, and typically allow experiments to be conducted over a 10° – 160° angular range.

6.3 Detector System

PMTs are almost universally used as detectors in DLS experiments (Table 3). These should have a low dark count and a high gain since most work is done in

Table 2 Summary of lasers commonly used in DLS installations

Type	Wavelength	Power	Size	Cost
HeNe	632.8 nm	5–35 mW	0.40–1.5 m	\$500–\$7000
Laser diodes	635–780 nm	5–100 mW	0.05–0.15 m	\$300–\$1200
Ar ⁺ (air cooled)	488–514.5 nm	~100 mW	1 m	\$8000
Ar ⁺ (water cooled)	488–514.5 nm	~1.7 W	1.5–2 m	\$16 000–\$40 000
DPSS (Frequ. Doubled)	532 nm	10 mW–4 W	0.2–0.5 m	\$3000–\$40 000

DPSS, diode pumped solid-state lasers.

Table 3 Summary of PMTs commonly used in DLS

Type	Photo cathode	Dynodes (gain)	Dark count/Max. count	Comment
EMI 9863B	S20	14 (10^7)	40 cps/5 Mc	Red sensitive, QE: 3–4%
EMI 9130	S20	11 (10^6)	40 cps/1 Mc	Red sensitive small tube
Ham R464	Bialkali	12 (6×10^6)	5 cps/2 Mc	Quartz window for UV
Ham R585	Bialkali	12 (6×10^6)	5 cps/2 Mc	Blue-green sensitive only
Ham R649	S20	12 (6×10^6)	200 cps/2 Mc	Red sensitive, QE: 3–4%
Ham HC120	S20	10 (10^6)	100 cps/2 Mc	Red sensitive, QE: 3–4%
SPCM	APD	NA (10^4)	500 cps/1 Mc	QE (635 nm): 35–70%

NA, not applicable

the single photon counting regime. A comparatively new development is the single photon counting mode (SPCM) by EG&G⁽⁵⁵⁾ which incorporates an avalanche photo diode (APD), active reset and quenching electronics and a Peltier-type temperature controller in a small package. This author investigated the properties of the APD (supplied then by RCA Canada) in 1985 and found that they were not well suited for DLS applications owing to the lack of active quenching and the lack of an integrated temperature control for the semiconductor junction (unpublished). Brown⁽⁵⁶⁾ developed the required circuits and successfully implemented APDs into small fiber-optic-based DLS devices. New SPCMs can replace PMTs in many applications, particularly for wavelengths of more than 680 nm (near infrared).

6.4 The Digital Correlator

The correlator has become the device of choice to generate the raw data in a DLS experiment, although the early experiments mostly employed “wave analyzers” or “spectrum analyzers”. (Today only one commercial instrument⁽³²⁾ still performs DLS particle sizing in the frequency domain by employing a real-time spectrum analyzer.) The basic design of a correlator is really very simple and was originally used at the Royal Radar Establishment, UK⁽⁵⁷⁾ (now Defence

Evaluation and Research Agency) to recover radar signals that are deeply buried in noise. This instrument was commercialized by (then) Precision Devices, (now) Malvern Instruments,⁽⁵⁸⁾ in the early 1970s. The ACF is formed by recording the number of photons arriving in each sample time, maintaining a history of this signal over a large range of sample times (time series), multiplying the instantaneous and the delayed signal for a range of time delays t_d (the “channels”) and accumulating these products. In the past most designs employed a multibit shift register to maintain a record of photon counts, as shown in Figure 4. In modern non-linear correlators shift registers have been replaced by fast memories, allowing very flexible channel configurations with dynamic ranges that exceed 10 decades of time. Individual design details may be gathered from the manufacturers’ literature.

Figure 5 shows an example of a complete stand-alone DLS-based, commercially available instrument that incorporates all of the above mentioned optics, electronics and data processing.

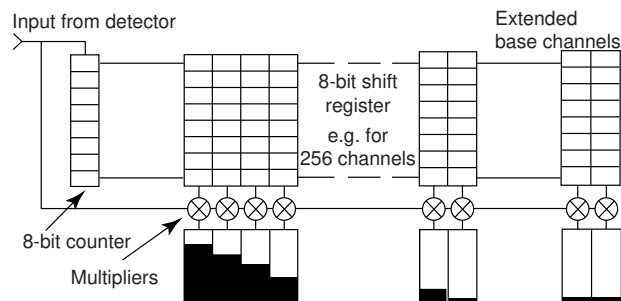


Figure 4 Block diagram of an 8-bit shift register digital correlator.



Figure 5 A typical DLS-based particle sizer. (Courtesy of Brookhaven Corp.)

7 EXAMPLES OF DYNAMIC LIGHT SCATTERING MEASUREMENTS

7.1 Particle Size Distributions

The majority of applications for DLS in particle sizing are the rapid routine measurements of mean sizes in QC work. Manufacturers of latexes, pigments, emulsions, micelles, liposomes, vesicles, sils and silica can track the consistency of the desired particle sizes rapidly and accurately, independent of different operators and different instruments anywhere in the world. Often a bimodal distribution characterizes a sample better and is actually expected from the known chemistry of the sample. In such cases $G(\Gamma)$ will contain two modes that can be separated if their size ratio is at least 1:2 and the relative intensities are similar. Samples that tend to coagulate are easily tracked by DLS. Although the exact size distribution cannot be determined, the first and second moments are very sensitive to any changes in the distribution and give an immediate and accurate response. DLS-based particle sizing is also widely used for biological samples such as bacteria, viruses, proteins, DNA, etc. Many applications are in crystal growth and polymer research. The following few examples illustrate the breadth of DLS-based size measurements.

- Spontaneous vesicle formation in a biological surfactant (ganglioside GM3) was investigated by L. Cantu and M. Corti.⁽⁵⁹⁾
- Studies of BSA and lysozyme, very low molecular weight proteins, were conducted by H. Dhadwal et al.⁽⁶⁰⁾
- Protein (lysozyme) crystallization was investigated by Mikol et al.⁽⁶¹⁾
- Submicron emulsion systems were measured by Herb et al.⁽⁶²⁾
- Liposome production is monitored by DLS in QC and research by the Avestin Corp.⁽⁶³⁾

- B. Weiner⁽⁴⁴⁾ et al. used a fiber optic backscattering device to observe particle–particle interaction in highly concentrated latex suspension.
- Particle sizing related research on non-ergodic systems have been published by van Megen.⁽⁶⁴⁾ DLS was applied to the glass phase of nonaqueous suspensions of sterically stabilized colloid spheres.
- A widely used industrial process, hydro metallurgical solvent extraction, was investigated by Neuman⁽⁶⁵⁾ et al., applying the DLS technique to very small particles in the region of 2 nm.
- Caldwell⁽⁶⁶⁾ investigated emulsions by employing DLS and sedimentation field flow fractionation (SFFF) methods in a complementary mode. SFFF provides for a high-resolution fractionation of the sample and DLS measures the sizes without the need to know the density of the sample.
- Multiangle particle sizing and its associated data transformation have been investigated by Cummins.⁽⁶⁷⁾ If the sample is very clean, the multiangle constraint can be a powerful conditioning for the inversion matrix to stabilize the set of $G(\Gamma)$.
- Auweter et al.⁽⁶⁸⁾ published on-line measurements with a one-fiber backscattering device as early as 1985. Their experiments demonstrated the feasibility of such fiber optics in a hostile environment.

8 COMPARISON WITH OTHER PARTICLE SIZING METHODS

Different techniques yield different “sizes” for the same particles simply because they employ different physics for the measurement. DLS, for example, will easily detect a few large particles among many small ones. Also, the DLS technique is *absolute* and there are no adjustable parameters available for a “calibration”. Often the term

Table 4 Comparison of particle sizing techniques

Technique	Resolution	Dyn. range	Calibration	Mass balance	Time/Sec
DLS (PCS)	Low	1 : 1000	Not required	Intrinsic	2–15
Particle counters	Very high	1 : 10	Required	Must be verified	8–20
Microscopes	Very high	1 : 10	Required	Not verifiable	>30
Laser diffraction	Low	1 : 300	Not required	Intrinsic	2–5
SLS (Mie)	Low	1 : 10	Required	Intrinsic	2–5
Time of transition	High	1 : 10	Required	Must be verified	8–30
Sedimentation	Very high	1 : 30	Not required	Intrinsic	5–30
Centrifugation	Very high	1 : 30	Not required	Intrinsic	5–30
SFFF	Very high	1 : 100	Not required	Must be verified	8–20
HDC	Very high	1 : 10	Required	Must be verified	8–20

HDC, hydrodynamic chromatography.

“calibration” is confused with the “validation”. As with any instrument, its proper operation must be verified with known samples, but no adjustments for calibration can be utilized to achieve the “correct” result. This is in contrast to microscopes or “particle counters” for which a calibration must be performed (Table 4).

Dynamic ranges are valid for one measurement without changing optics, capillaries, etc. All the techniques cover at least part of the DLS range of particle sizes: ca. 0.001–3 μm . Measurement times are typical and depend on the breadth of the distribution, absolute size and physical properties of the particles (e.g. density), desired precision, etc. The widely used Fraunhofer diffraction instruments are advertised as covering a size range of as low as 20 nm to several millimeters. These devices actually combine two distinct instruments: one that is based on diffraction theory (low-angle scattering) with d^2 weighting and one based on Mie scattering with d^6 weighting. This explains the large dynamic range that is advertised for these instruments but because of the different weighting and low resolution a true merging of the mass distribution is impossible, regardless of the claims in the manufacturers’ literature. Thus comparisons between DLS and “Fraunhofer” sizing results ought to be performed with great caution by carefully evaluating the experimental conditions and examining the mathematical transformations that are required.

9 NEW DEVELOPMENTS

9.1 New Correlator Developments

In the last several years new correlators have become available, which are remarkably compact, have a large dynamic range in delay time and can accommodate many more counts in a given sample time. These developments are a direct result of the availability of more versatile, higher speed and higher density integrated circuits, and novel approaches to the implementation of the autocorrelation operation. Based on designs by K. Schätzel^(22,23) the ALV company⁽⁶⁹⁾ is developing a correlator with 16 inputs and a minimum sample time of 800 nsec (50 nsec for a single input). Brookhaven⁽⁷⁰⁾ is developing a new correlator that incorporates sophisticated multiple digital signal processing (DSP) in real time. Flexible Instruments⁽⁷¹⁾ offers a range of application-specific integrated circuits based correlator boards. Correlators are really nothing more than specialized DSP instruments, regardless of their specific designs. As such the design of these devices benefits from the relentless improvement in the semiconductor industry: higher speed, more integration, lower power, physically smaller and higher gate densities. These

new correlators will extend the application of DLS and improve existing applications.

9.2 Solid-state Lasers

These diodes have become reliable and stable enough to be used in routine DLS based measurements. Higher power DPSS lasers are beginning to replace Ar⁺ in many installations. Near infrared lasers (>780 nm) at 100 mW and more can be used in combination with APDs⁽⁵⁵⁾ and are particularly well suited for efficient coupling into single-mode fiber optics (large wavelength).

9.3 Fiber Optics

Bulk optics are being replaced more and more with fiber-optic devices. Ricka⁽⁷²⁾ has shown that single-mode fibers have the unique property of acting as spatial filters yielding high ACF intercepts near the theoretical maximum without sacrificing high intensities that are received by the detector. Ongoing developments will improve the efficiency of launching laser beams into single-mode fibers (currently about 40%) and make polarization-preserving filters more widely available.

9.4 New Applications

- Diffusing wave spectroscopy (DWS): in these new experiments by D. Pine and D. Weitz⁽⁷³⁾ a “length parameter” is calculated from the initial fast decay of the ACF from multiple scattered light, extending DLS applications to samples with higher particle concentrations.
- W. Meyer et al.^(74,75) at the National Aeronautics and Space Administration (NASA) designed a promising set-up that employs two detectors and two single mode fibers that are located a tiny distance apart such that the scattered light originates most likely from one speckle. The cross correlation function (CCF) of the signals from the two detectors yields the proper D_T and hence particle size.
- Based on original work by Dhadwal et al.,⁽⁷⁶⁾ the commercially available FOQELS instrument from Brookhaven Instruments Corp.⁽⁷⁰⁾ utilizes two single-mode fibers at a 155° backscattering angle.
- ALV⁽⁶⁹⁾ is currently developing a dual-fiber instrument for backscattering at a 173° angle.

Continuing development of fiber-optic technology will make it possible to construct compact, multiangle light-scattering spectrometers for DLS (and SLS) with no moving parts.

10 CONCLUSION

As any other particle sizing technique, DLS has advantages and disadvantages and it is particularly important to use it strictly within the framework of physical laws, if meaningful results are to be obtained. The following is a short compilation of the advantages and disadvantages of DLS-based particle sizing.

10.1 Disadvantages

- It does not produce a high-resolution histogram of the size distribution.
- Like other nonimaging techniques an equivalent sphere diameter is usually, although not always, assumed. Shape information is not easily obtained.
- When proper measurements are made, the parameters which are most often obtained are the inverse z -average moments of the size distribution, not the usually reported parameters of a size distribution.
- Dust can make measurement and interpretation difficult.

10.2 Advantages

- Measurements are fast, from seconds to minutes.
- The technique is absolute, from first principles. Calibration with a known size distribution is not necessary to get answers.
- Very small quantities of sample can be measured.
- Any suitable suspending liquid can be used provided it is nonabsorbing, relatively clear and not too viscous.
- The technique is applicable from about 0.001 to several microns.
- Instrumentation is commercially available for both research and QC measurements with automation including data analysis.
- Although the interpretation of particle size is least ambiguous with a narrow distribution, an effective diameter and polydispersity index are measurable even with broad distributions.

In order to provide an introduction to the DLS technique, the physical basis of the technique and the associated instrumentation has been discussed. Several new developments in the instrumentation have been described which have the potential for fundamentally changing the way DLS measurements are made and lead to many new applications of the technique. The commercial importance of DLS as a submicrometer particle sizing tool ensures that technological developments will occur rapidly in this field.^(32,55,58,63,69,70,71,77–79)

LIST OF SYMBOLS

a	Instrument constant
A_{coh}	Coherence area
A_{det}	Detector area
A/D	Amplifier/Discriminator
Ar^+	Argon Ion laser
B	Baseline of the intensity ACF $G^{(2)}(t_d)$ before normalization
$B(c)$	Concentration factor
c	Particle concentration
cps	Photon counts per second
$g^{(1)}(t_d)$	Normalized correlation coefficient at delay t_d (Field ACF)
d	Particle diameter
d_{det}	Diameter of the detector area
$\langle d_n \rangle$	Mean diameter by number
d_p	Distance between particles
d_{sr}	Diameter of scattering area
dz	z -average diameter (the next higher weighting after mass: intensity)
D_T	Translational diffusion coefficient
$g^{(1)}(t_d)$	First-order correlation coefficient at delay t_d
$G(\Gamma)$	Line width distribution function
HeNe	Helium Neon laser
$\langle I(q) \rangle$	Time averaged intensity at wave vector q
k_B	Boltzman constant
K	Optical constant
M	Particle mass
n	Refractive index
N	Number of particles
$P(\Theta)$	Particle form factor
q	Wave vector
Q	Polydispersity index
R	Distance between scattering volume and detector
t	Time
t_d	Delay time between multiplication terms for $C(t_d)$
T	Absolute temperature (Kelvin)
Γ	Line width of scattered light (radians/sec)
$\langle \Gamma \rangle$	Average line width
$\eta(T)$	Viscosity of the medium in which particles are suspended (Poise)
Θ	Scattering angle
λ	Wavelength of light in the suspension medium (λ_0/n)
λ_0	Wavelength of light in vacuo
μ_i	Moments of a distribution ($i = 1, 2, \dots$)
τ	Decay constant for exponential forms of $C(t_d)$; $C(\tau) = C(0)/e$

ABBREVIATIONS AND ACRONYMS

ACF	Auto Correlation Function
APD	Avalanche Photo Diode
CCF	Cross Correlation Function
DLS	Dynamic Light Scattering
DPSS	Diode Pumped Solid-state Lasers
DSP	Digital Signal Processing
DWS	Diffusing Wave Spectroscopy
HDC	Hydrodynamic Chromatography
IFS	Intensity Fluctuation Spectroscopy
ISO	International Organization for Standardization
NASA	National Aeronautics and Space Administration
NNLS	Non-negative Least Square
PCS	Photon Correlation Spectroscopy
PMT	Photo Multiplier Tube
QC	Quality Control
QE	Quantum Efficiency
QELS	Quasi-elastic Light Scattering
SFFF	Sedimentation Field Flow Fractionation
SLS	Static Light Scattering
S/N	Signal-to-noise Ratio
SPC	Statistical Process Control
SPCM	Single Photon Counting Mode
TEM	Transmission Electron Microscope

RELATED ARTICLES

Particle Size Analysis (Volume 6)

Particle Size Analysis: Introduction • Diffraction in Particle Size Analysis • Electrozone Sensing in Particle Size Analysis • Field-flow Fractionation in Particle Size Analysis • Light Scattering, Classical: Size and Size Distribution Characterization • Optical Particle Counting • Sedimentation in Particle Size Analysis • Ultrasonic Measurements in Particle Size Analysis • Velocimetry in Particle Size Analysis

Polymers and Rubbers (Volume 8)

Polymers and Rubbers: Introduction

Polymers and Rubbers cont'd (Volume 9)

Field Flow Fractionation in Analysis of Polymers and Rubbers • Neutron Scattering in Analysis of Polymers and Rubbers

General Articles (Volume 15)

Analytical Problem Solving: Selection of Analytical Methods

REFERENCES

1. S.P. Lee, W. Tscharnuter, B. Chu, 'Calibration of an Optical Self-beating Spectrometer by Polystyrene Latex Spheres, and Confirmation of the Stokes–Einstein Formula', *J. Polym. Sci.*, **10**, 2453 (1972).
2. J. Tyndall, 'On the Blue Color of the Sky, the Polarization of the Skylight and on the Polarization of Light by Cloudy Matter Generally', *Phil. Mag.*, **37**, 384–394 (1869).
3. M. Kerker, *The Scattering of Light and Other Electromagnetic Radiation*, Academic Press, New York, 1969.
4. Lord Rayleigh, 'On the Electromagnetic Theory of Light', *Philos. Mag.*, **12**, 81–101 (1881).
5. A. Einstein, 'Theorie der Opaleszenz von homogenen Flüssigkeitsgemischen in der Nähe des kritischen Zustandes', *Annalen der Physik*, **33**, 1275 (1910).
6. B.J. Berne, R. Pecora, *Dynamic Light Scattering*, Wiley-Interscience, New York, 1976.
7. H.Z. Cummins, E.R. Pike (eds.), *Photon Correlation and Light Beating Spectroscopy*, Plenum Press, New York, 1974.
8. H.Z. Cummins, E.R. Pike (eds.), *Photon Correlation Spectroscopy and Velocimetry*, Plenum Press, New York, 1977.
9. B. Chu, *Laser Light Scattering*, Academic Press, New York, 1974.
10. S.H. Chen, B. Chu, R. Nossal (eds.), *Scattering Techniques Applied to Supramolecular Systems*, Plenum Press, New York, 1981.
11. R. Pecora (ed.), *Dynamic Light Scattering – Applications of Photon Correlation Spectroscopy*, Plenum Press, New York, 1985.
12. B.E. Dahneke (ed.), *Measurement of Suspended Particles by Quasi-elastic Light Scattering*, Wiley-Interscience, New York, 1983.
13. K.S. Schmitz, *An Introduction to Dynamic Light Scattering by Macromolecules*, Academic Press, New York, 1990.
14. G.D.J. Phillies, 'Quasielastic Light Scattering', *Anal. Chem.*, **62**(20), 1049A–1057A (1990).
15. B. Chu, 'Advances in Methods of Light Scattering Spectroscopy', *Pure and Appl. Chem.*, **49**, 941–962 (1977).
16. V.A. Bloomfield, 'Quasielastic Light Scattering Applications in Biochemistry and Biology', *Ann. Rev. Biophys. Bioeng.*, **10**, 421–450 (1981).
17. F.D. Carlson, 'The Application of Intensity Fluctuation Spectroscopy to Molecular Biology', *Ann. Rev. Biophys. Bioeng.*, **4**, 243–264 (1975).
18. W.H. Flygare, 'Light Scattering in Pure Liquids and Solutions', *Chem. Soc. Rev.*, **6**, 109–137 (1977).
19. P.N. Pusey, J.M. Vaughan, 'Light Scattering and Intensity Fluctuation Spectroscopy', in *Dielectric and Related Processes*, ed. M. Davies, Chemical Society, London, Vol. 2, 1975.

20. J.M. Schurr, 'Dynamic Light Scattering of Biopolymers and Biocolloids', *CRC Crit. Rev. Biochem.*, **4**, 371–431 (1977).
21. I.W. Shepherd, 'Inelastic Laser Light Scattering from Synthetic and Biological Polymers', *Rep. Prog. Phys.*, **38**, 565–630 (1975).
22. K. Schätzel, 'Correlation Techniques in Dynamic Light Scattering', *Appl. Phys. B.*, **42**, 193–213 (1987).
23. K. Schätzel, M. Drewel, Sven Stimac, 'Photon correlation measurements at large lag times: improving statistical accuracy', *J. Modern Optics*, **35**(4), 711–718 (1988).
24. B. Chu (ed.), 'Selected Papers on Light Scattering by Macromolecular, Supramolecular and Fluid Systems', SPIE Optical Engineering Press, Bellingham, WA, 1990.
25. N.C. Ford, 'Theory and Practice of Photon Correlation Spectroscopy', in *Measurement of Suspended Particles by Quasi-elastic Light Scattering*, ed. B.E. Dahneke, Wiley-Interscience, New York, 1983.
26. W. Brown, *Dynamic Light Scattering*, Clarendon Press, Oxford, 210–211, 1993.
27. R. Pecora, 'Doppler Shifts in Light Scattering from Pure Liquids and Polymer Solutions', *J. Chem. Phys.*, **40**, 1604–1614 (1964).
28. M. Bertero, P. Boccacci, E.R. Pike, 'On the Recovery and Resolution of Exponential Relaxation Rates from Experimental Data: A Singular-value Analysis of the Laplace Transform Inversion in the Presence of Noise', *Proc. Royal Soc. London*, **A383**, 15–29 (1982).
29. M. Bertero, P. Boccacci, E.R. Pike, 'On the Recovery and Resolution of Exponential Relaxation Rates from Experimental Data. II. The Optimum Choice of the Sampling Points', *Proc. Royal Soc. London*, **A393**, 51–65 (1984).
30. H.Z. Cummins, N. Knable, Y. Yeh, 'Observation of Diffusion Broadening of Raleigh Scattered Light', *Phys. Rev. Lett.*, **12**, 150–153 (1964).
31. N.C. Ford, 'Theory and Practice of Photon Correlation Spectroscopy', in *Measurement of Suspended Particles by Quasi-elastic Light Scattering*, ed. B.E. Dahneke, Wiley-Interscience, New York, 1983.
32. Honeywell IAC (Microtrac), 1100 Virginia Dr., Fort Washington, PA 19034, USA.
33. P.N. Pusey, in *Photon Correlation Spectroscopy and Velocimetry*, ed. H.Z. Cummins, E.R. Pike, Plenum, New York, 1977.
34. R.J. Glauber, 'Coherent and Incoherent States of the Radiation Field', *Phys. Rev.*, **131**, 2766–2788 (1963).
35. A.J.F. Siegert, 'On the Fluctuations in Signals Returned by many Independently Moving Scatterers', Massachusetts Institute of Technology, Boston, MA, M.I.T. Rad. Lab. Rep., No. 465, 1943.
36. C. Tanford, *Physical Chemistry of Macromolecules*, J. Wiley and Sons, New York, 1957.
37. H.Z. Cummins, F.D. Carlson, T.J. Herbert, G. Woods, 'Translational and Rotational Diffusion Constants of Tobacco Mosaic Virus from Rayleigh Line Widths', *Biophys. J.*, **9**, 518 (1969).
38. B. Chu, Es. Gulari, Er. Gulari, 'Details of Histogram Approach and Comparison of Methods of Data Analysis', *Phys. Scr.*, **19**, 476 (1979).
39. J.G. McWhirter, E.R. Pike, 'Numerical Inversion of Laplace Transform and Similar Fredholm Integral Equation of 1st Kind', *J. Phys. A: Math. Gen.*, **11**, 1729 (1978).
40. J.G. McWhirter, 'A Stabilized Model-fitting Approach to the Processing of Laser Anemometry and other Photon-correlation Data', *Opt. Acta*, **27**, 83 (1980).
41. N. Ostrowsky, D. Sornett, P. Parker, E.R. Pike, 'Exponential Sampling Method for Light-scattering Polydispersity', *Opt. Acta*, **28**, 1059 (1981).
42. S.W. Provencher, J. Hendrix, L. De Maeyer, N. Paulussen, 'Direct Determination of Molecular-Weight Distributions of Polystyrene in Cyclohexane with Photon Correlation Spectroscopy', *J. Chem. Phys.*, **69**, 4273 (1978).
43. S.W. Provencher, 'Inverse Problems in Polymer Characterization: Direct Analysis of Polydispersity with Photon Correlation Spectroscopy', *Macromol. Chem.*, **180**, 201 (1979).
44. B. Weiner, W. Tscharnuter, A. Banerjee, 'Developing Fiber Optic Probes for Noninvasive Particle Size Measurements in Concentrated Suspensions using DLS. Or, How to Make a Zero Shear Rheometer without Really Trying', Brookhaven Corp. Internal Memorandum, 1996.
45. S.F. Gull, *Developments in Maximum Entropy Data Analysis*, Kluwer Academic, Norwell, MA, 53–71, 1989.
46. J. Jakes, 'Testing of the Constrained Regularization Method of Inverting Laplace Transform on Simulated very wide Quasi-elastic Light Scattering Auto-Correlation Functions', *Czech. J. Phys.*, **38**, 1305 (1988).
47. Chris De Vos, Luc Deriemaeker, Robert Finsy, 'Quantitative Assessment of the Conditioning of the Inversion of Quasi-elastic and Static Light Scattering Data for Particle Size Distributions', *Langmuir*, **12**, 2630–2636 (1996).
48. Robert Finsy, 'Particle Sizing by Quasi-elastic Light Scattering', *Adv. Coll. Interf. Sci.*, **52**, 79–143 (1994).
49. H. Ruf, E. Grell, E.H.K. Stelzer, 'Size Distribution of Submicron Particles by Dynamic Light Scattering Measurements: Analyses Considering Normalization Errors', *Eur. Biophys. J.*, **21**, 21–28 (1992).
50. J.C. Brown, P.N. Pusey, R. Dietz, 'Photon Correlation Study of Polydisperse Samples of Polystyrene in Cyclohexane', *J. Chem. Phys.*, **62**, 1136 (1975).
51. D.E. Koppel, 'Analysis of Macromolecular Polydispersity in Intensity Correlation Spectroscopy: The Method of Cumulants', *J. Chem. Phys.*, **57**, 4814 (1972).
52. John C. Thomas, 'The Determination of Log Normal Particle Size Distributions by Dynamic Light Scattering', *J. Coll. Interf. Sci.*, **117**(1) (1987).
53. R.J. Hunter, *Zeta Potential in Colloid Science, Principles and Applications*, Academic Press, London, 17–21, 1981.
54. ISO document, 'Particle Size Analysis – Photon Correlation Spectroscopy', Draft International Standard ISO/DIS 13321, ICS 19.120.00, 1994.

55. EG&G Electro Optics, P.O.Box 900, Vaudreuil J7V 7X3, Canada.
56. R.G.W. Brown, J.G. Burnett, J. Mansbridge, C.I. Moir, 'Miniature Laser Light Scattering Instrumentation for Particle Size Analysis', *Appl. Opt.*, **29**, 4159–4169 (1990).
57. E. Jakeman, R. Jones, C.J. Oliver, E.R. Pike, 'Optical Signal Processing', Royal Radar Establishment, Ministry of Defence, Malvern, Worcs, UK, RRE Memorandum, No. 2621, 1970.
58. Malvern Instruments Ltd., Malvern, Worcestershire, UK.
59. L. Cantu, M. Corti, M. Musolino, P. Salina, 'Spontaneous Vesicle Formation from a One-component Solution of a Biological Surfactant', *Progr. Colloid. Polym. Sci.*, **84**, 21–23 (1991).
60. H.S. Dhadwal, William W. Wilson, Rafat R. Ansari, William V. Meyer, 'Dynamic Light Scattering Studies of BSA and Lysozyme Using a Backscatter Fiber Optic System', Proceedings Static and Dynamic Scattering in Medicine and Biology, Society of Photo-optical Instrumentation Engineers, Bellingham, WA 98227, SPIE Vol. 1884, 1993.
61. V. Mikol, E. Hirsch, R. Giege, 'Monitoring Protein Crystallization by Dynamic Light Scattering', *FEBS Lett.*, **258**(1), 63–66 (1989).
62. C.A. Herb, E.J. Berger, K. Chang, I.D. Morrison, E.F. Grabowski, 'Using Quasi-elastic Light Scattering to Study Particle Size Distributions in Submicrometer Emulsion Systems', ACS Symposium Series No. 332, 1987.
63. Avestin Inc., 2450 Don Reid Drive, Ottawa K1H 8P5, Canada.
64. W. van Megen, S.M. Underwood, 'Dynamic-light-scattering Study of Glasses of Hard Colloid Spheres', *Phys. Rev. E*, **47**(1), 248–261 (1993).
65. Ronald D. Neuman, M.A. Jones, Nai-Fu Zhou, 'Photon Correlation Spectroscopy Applied to Hydro Metallurgical Solvent Extraction Systems', *Coll. Surf.*, **46**, 45–64 (1990).
66. Karin D. Caldwell, Jianmin Li, 'Emulsion Characterization by the Combined Sedimentation Field-flow Fractionation-Photon Correlation Spectroscopy Methods', *J. Coll. Interf. Sci.*, **132**(1), 256–268 (1989).
67. P.G. Cummins, E.J. Staples, 'Particle Size Distributions Determined by a "Multi angle" Analysis of Photon Correlation Spectroscopy Data', *Langmuir*, **3**, 1109–1113 (1987).
68. H. Auweter, D. Horn, 'Fiber-optical Quasi-elastic Light Scattering of Concentrated Dispersions', *J. Coll. Interf. Sci.*, **105**(2), 399–409 (1985).
69. Allgemeine Laser Vertriebsgesellschaft mbH, Robert-Bosch-Str. 9, D-63225 Langen, Germany.
70. Brookhaven Instruments Corp., 750 Blue Point Road, Holtville, NY 11766, USA.
71. Flexible Instruments, 15 Colmart Way, Bridgewater, NJ 08807, USA.
72. J. Ricka, 'Brownian Dynamics in Strongly Scattering Porous Media – Dynamic Light Scattering with Single-mode Matching', *Macromol.*, **79**, 45–55 (1994).
73. D.J. Pine, D.A. Weitz, P.M. Chaikin, E. Herbolzheimer, 'Diffusing-wave Spectroscopy', *Phys. Rev. Lett.*, **60**(12), 1134–1137 (1988).
74. William V. Meyer, David S. Cannell, Anthony E. Smart, Thomas W. Taylor, Padetha Tin, 'Multiple Scattering Suppression by Cross-correlation', Applied Optics, L.P.E. Div., Photon Correlation & Scattering, 1997.
75. W.V. Meyer, W.W. Tscharnuter, A.D. MacGregor, H. Dauter, P. Deschamps, F. Boucher, J. Zhu, P. Tin, R.B. Rogers, R.R. Ansari, 'Laser Light Scattering, From an Advanced Technology Development Program to Experiments in a Reduced Gravity Environment', International Symposium on Space Optics, Garmisch-Partenkirchen, Germany, EOS/SPIE Joint Venture, paper 2210-2221, April 18–22, 1994.
76. Harbans S. Dhadwal, Rafat R. Ansari, William V. Meyer, 'A Fiber-optic Probe for Particle Sizing in Concentrated Suspensions', *Rev. Sci. Instrum.*, **62**(12), 2963–2968 (1991).
77. Coulter Beckman Corp., P.O. Box 169015, Miami, FL 33116-9015, USA.
78. Particle Sizing Systems, 75 Aero Camino, Santa Barbara, CA 93117, USA.
79. Protein Solutions, Inc., 1224 West Main Street, Suite 777, Charlottesville, VA 22903.